NUCL SCI TECH (2017) 28:55
DOI 10.1007/s41365-017-0207-x

Production of light nuclei and hypernuclei at High Intensity Accelerator Facility energy region

Peng Liu[1,2] · Jin-Hui Chen[1] · Yu-Gang Ma[1] · Song Zhang[1]

Received: 13 November 2016 / Revised: 26 December 2016 / Accepted: 2 January 2017 / Published online: 3 March 2017

Abstract Heavy-ion collisions are powerful tools for studying hypernuclear physics. We develop a dynamical coalescence model coupled with an ART model (version 1.0) to study the production rates of light nuclear clusters and hypernuclei in heavy-ion reactions, for instance, the deuteron (d), triton (t), helium (^{3}He), and hypertriton ($^3_\Lambda$H) in minimum bias (0–80% centrality) ^{6}Li + ^{12}C reactions at beam energy of 3.5*A* GeV. The penalty factor for light clusters is extracted from the yields, and the distributions of θ angle of particles, which provide direct suggesetions about the location of particle detectors in the near future facility—High Intensity heavy-ion Accelerator Facility (HIAF) are investigated. Our calculation demonstrates that HIAF is suitable for studying hypernuclear physics.

The original version of this article is revised. In the original publication of this article equations. 1–7 and equation. 9 have been incorrectly online published. The correct version of the equations is updated in this original article.

This work was supported in part by the Major State Basic Research Development Program in China (Nos. 2014CB845401 and 2015CB856904), and the National Natural Science Foundation of China (Nos. 11421505, 11520101004, 11275250, 11322547 and U1232206), and Key Program of CAS for the Frontier Science (No. QYZDJ-SSW-SLH002).

✉ Jin-Hui Chen
chenjinhui@sinap.ac.cn

✉ Yu-Gang Ma
ygma@sinap.ac.cn

[1] Shanghai Institute of Applied Physics, Chinese Academy of Sciences, Shanghai 201800, China

[2] University of Chinese Academy of Sciences, Beijing 100049, China

Keywords Heavy-ion accelerator facility · Hyperon · Hypernuclei · Coalescence · Light nuclei

1 Introduction

Hypernuclei consists of nuclei and one or more hyperons in which at least one quark is strange quark or anti-strange quark. Hypernuclear physics is a fascinating and a fundamental interesting field. It has been studied for many years, and more exotic forms of multistrange nuclear systems have been hypothesized to exist [1]. In particular, the hyperon–nucleon (YN) and hyperon–hyperon (YY) interactions play a fundamental role in the softening of the equation of state (EOS) of neutron stars [2]. Studying YN/YY interactions will help us to understand the hyperon puzzle that microscopic EOS for hyperomic matter is very soft and is not compatible with the measured neutron stars masses. Understanding the structure of neutron stars requires more information on the YN/YY interaction knowledge. For example, depending on the strength of the YN interaction, the collapsed stellar core could consist of hyperons, strange quark matter, or a kaon condensate [3]. The lifetimes of the hypernucleus depend on the strength of the YN interaction [4, 5], therefore, a precise determination of the lifetimes of hypernuclei provides direct information on the YN interaction strength [5, 6].

Many models, including quark-gluon plasma distillation, thermal production, and coalescence mechanism, have been developed to understand the hypernuclei production mechanism in heavy-ion collisions. In this paper, a dynamical coalescence model, in which the probabilities of the overlapping of the wave functions between nucleons and hyperons at the final stage of the collisions determine the formation of hypernuclei [7], was developed to study

the formation of hypernuclei production. Additionally, the ART model was used to simulate the interaction between hadrons produced at the final stage of a heavy-ion collision evolution. We will introduce the dynamical coalescence model and the ART model in detail in Sect. 2.

In a laboratory environment, heavy-ion collisions experiments provide a powerful tool for studying the properties of nuclear matter and the interactions between hadrons under the conditions of high temperature and baryon density [8–15]. Heavy-ion collisions may create plenty of hypernuclei and their anti-particles, for example, the ${}^{3}_{\Lambda}$H, anti-${}^{3}_{\Lambda}$H [16–19]. There are some surprising results about hypernuclear measurements in recent years. The STAR Collaboration at RHIC and the ALICE Collaboration at CERN reported a signal of (anti-)${}^{3}_{\Lambda}$H, respectively, plus the mass and the lifetime parameter [16–18]. In 2013, The GSI HypHI Collaboration reported measurement on the lifetime of ${}^{3}_{\Lambda}$H and ${}^{4}_{\Lambda}$H, produced by driving a ^{6}Li beam on a ^{12}C target at 2A GeV [19]. All new results show a shorter lifetime of ${}^{3}_{\Lambda}$H in comparison with the free Λ's. The physics origin is still under hot debate [20]. Neutron-Rich Λ-Hypernuclei, which have more neutrons in comparison with protons, for example the ${}^{6}_{\Lambda}$H, ${}^{7}_{\Lambda}$He, ${}^{9}_{\Lambda}$He, ${}^{10}_{\Lambda}$Li, ${}^{12}_{\Lambda}$Be and ${}^{16}_{\Lambda}$C, have been studied by KEK Collaboration, FINUDA Collaboration, and JLab E01-011 experiment [21].

Many new proposals on hypernucleus physics are raised in the field, such as the new forms of nuclear bound systems including a multistrange hyperon, the double Ξ or double Ω [22], are waiting to be discovered. Hypernucleus measurement is very useful to check the production mechanism. For instance, is it due to nucleonic (hyperon) coalescence [23] or other direct formation mechanism etc? Due to the low statistics and limited resolution on the detector, the early measurements on light hypernuclei systems usually have a large statistical uncertainty. The next generation facilities of heavy-ion collisions aimed at the hypernuclear physics should improve the detector resolution and the statistics to achieve a conclusive measurement. In this perspective, the Japan Proton Accelerator Research Complex (J-PARC) and the Nuclear Spectroscopic Telescope Array (NuSTAR) in America have been developed to study hypernuclear physics. Facility for Antiproton and Ion Research in Europe (FAIR) is under construction. In China, the High Intensity Accelerator Facility (HIAF) construction starting in late 2015 and will be built completely in about 2020. HIAF will produce the strongest beam intensity in the world when it is completed, and we will obtain more data to improve the statistics for hypernuclear physics study. In this paper, the ART model coupled with a dynamical coalescence is developed to simulate the collisions of a ^{6}Li beam with energy of 3.5A GeV (which is at the HIAF energy region) on a ^{12}C target collision. The light hypernuclei yields are calculated and the results prove that HIAF is suitable for studying the physics of the light hypernuclei system.

2 Introduction to ART 1.0 model

Relativistic transport model (ART 1.0), that is based on the well-known Boltzmann-Uehling-Uhlenbeck(BUU) model [24, 25] for intermediate energy heavy-ion collisions, was originally developed for the heavy-ion collisions at the alternating gradient synchrotron (AGS) energies [26]. ART 1.0 include the baryons N, $\Delta(1232)$, $N^*(1440)$, $N^*(1535)$, Λ, Σ, and mesons π, ρ, ω, η, K, as well as their explicit isospin degrees of freedom [27]. Both elastic and inelastic interaction between baryon and baryon, baryon and hyperon, and hyperon and hyperon are included in ART 1.0 model, almost all parametrised cross sections and angular distributions that have been used in the BUU model are replaced by empirical expressions based on the double-logarithmic interpolations of the experimental data [27]. Most inelastic scattering between hadron and hadron collisions are modeled through the formation of resonances.

For the inelastic baryon-baryon interactions, ART 1.0 includes the following inelastic channels [26]:

$$NN \leftrightarrow N(\Delta N^*), \tag{1}$$

$$NN \leftrightarrow \Delta(\Delta N^*(1440)), \tag{2}$$

$$NN \leftrightarrow NN(\pi\rho\omega), \tag{3}$$

$$(N\Delta)\Delta \leftrightarrow NN^*, \tag{4}$$

$$\Delta N^*(1440) \leftrightarrow NN^*(1535). \tag{5}$$

In above equations, N^* denotes either $N^*(1440)$ or $N^*(1535)$, and the symbol (ΔN^*) denotes a Δ or an N^*. For meson-baryon scatterings, ART 1.0 includes the following reaction channels for the formation and decay of resonances [26]:

$$\eta N \leftrightarrow N^*(1535), \tag{6}$$

$$\pi N \leftrightarrow \Delta, N^*(1440), N^*(1535). \tag{7}$$

The elastic scattering

$$(\pi\rho)(N\Delta N^*) \rightarrow (\pi\rho)(N\Delta N^*) \tag{8}$$

also is included in the ART 1.0 model. ART 1.0 model simulates π-π collision through the formation of a ρ meson, for example [27],

$$\pi + \pi \leftrightarrow \rho, \tag{9}$$

and the direct process

$$\pi + \pi \rightarrow \pi + \pi. \tag{10}$$

Λ hyperon production is mainly associated with a K^+ meson production through baryon-baryon collision [27],

$$NN \rightarrow N\Lambda(\Sigma)K, \Delta\Lambda(\Sigma)K, \tag{11}$$

$$NR \rightarrow N\Lambda(\Sigma)K, \Delta\Lambda(\Sigma)K, \tag{12}$$

$$RR \rightarrow N\Lambda(\Sigma)K, \Delta\Lambda(\Sigma)K, \tag{13}$$

where R denotes Δ, $N^*(1440)$, or $N^*(1535)$. The isospin-averaged cross sections for Λ production can be expressed as following [27]:

$$\begin{aligned}\bar{\sigma}\left(NN \rightarrow N\Lambda K^+\right) &\approx \bar{\sigma}(NN \rightarrow \Delta\Lambda K^+) \\ &\approx \frac{3}{2}\sigma\left(pp \rightarrow p\Lambda K^+\right).\end{aligned} \tag{14}$$

The threshold energies are 2.56, 2.74 for the final states $N\Lambda K$, $\Delta\Lambda K$, respectively. There is an approximation that the Λ production cross sections in reactions induced by resonances are the same as in nucleon-nucleon collisions at the same center-of-mass energy [27].

Meson-baryon interactions also can produce Λ hyperon production [27],

$$\pi + N(\Delta, N^*) \rightarrow \Lambda(\Sigma) + K, \tag{15}$$

$$\rho + N(\Delta, N^*) \rightarrow \Lambda(\Sigma) + K, \tag{16}$$

$$\omega + N(\Delta, N^*) \rightarrow \Lambda(\Sigma) + K. \tag{17}$$

For pion-nucleon collisions, the isospin-averaged cross sections for Λ production can be expressed as following [27]:

$$\bar{\sigma}(\pi N \rightarrow \Lambda K^+) \approx \frac{1}{4}\sigma(\pi^+ n \rightarrow \Lambda K^+). \tag{18}$$

In the $\rho + N$ and $\omega + N$ collisions, the cross sections for Λ production is taken for simplicity to be the same as in the $\pi + N$ collision at the same center-of-mass energy [27].

3 Introduction to a dynamical coalescence model

The dynamical coalescence model is a very popular method for describing the formation of cluster in heavy-ion collisions at both intermediate energies [28] and high energies [29–32]. The probability that hadrons form a cluster like deuteron and triton, is determined by the overlapping of the wave functions of coalescing hadrons with the internal wave function of the cluster [28, 30, 31]. In this model, assumptions about coalescing hadrons are statistically independent and the binding energy of formed cluster and the quantum dynamics of the coalescing process play only minor roles [30, 33]. We assume that correlations among hadrons that form the clusters are weak, and the binding energies of formed clusters can be neglected. In ART 1.0, simulations of heavy-ion collisions, the multiplicity of a M-hadron cluster produced by the dynamical coalescence model in heavy-ion collisions, is given by the following formula [33–35],

$$\begin{aligned}N_M = G \int & \mathrm{d}\mathbf{r}_{i_1}\mathrm{d}\mathbf{q}_{i_1}\cdots\mathrm{d}\mathbf{r}_{i_{M-1}}\mathrm{d}\mathbf{q}_{i_{M-1}} \\ & \times \left\langle \sum_{i_1 > i_2 > \cdots > i_M} \rho_i^W\left(\mathbf{r}_{i_1}, \mathbf{q}_{i_1}\cdots\mathbf{r}_{i_{M-1}}, \mathbf{q}_{i_{M-1}}\right)\right\rangle.\end{aligned} \tag{19}$$

In Eq. (19), $\mathbf{r}_{i_1},\ldots,\mathbf{r}_{i_{M-1}}$ and $\mathbf{q}_{i_1},\ldots,\mathbf{q}_{i_{M-1}}$ are, respectively, the $M-1$ relative coordinates and momenta in the M-hadron rest frame; ρ_i^W is the Wigner phase-space density of the M-hadron cluster, and $\langle\cdots\rangle$ denotes the event averaging. G represents the statistical factor for the cluster; it is 3/8 for d, 1/3 for t, ^{3}He [28, 30, 31, 36], and $^3_\Lambda$H [7].

To determine the hadron Wigner phase-space functions inside clusters, firstly the information about their hadron wave functions is required. For determining the wave functions of hadrons inside the clusters, we treat the cluster system as a spherical harmonic oscillator [28, 37]. Taking the above methods, we can get the hadrons wave functions inside the deuteron:

$$\psi(\mathbf{r}_1, \mathbf{r}_2) = 1/\left(\pi\sigma_\mathrm{d}^2\right)^{3/4}\exp\left[-\mathbf{r}^2/(2\sigma_\mathrm{d}^2)\right], \tag{20}$$

in terms of the relative coordinate $\mathbf{r} = \mathbf{r}_1 - \mathbf{r}_2$ and the size parameter σ_d. The root-mean-square radius can be deduced as $R_\mathrm{d} = \langle\mathbf{r}^2\rangle^{1/2} = (3/8)^{1/2}\sigma_\mathrm{d}$ for deuteron. Then, the hadron Wigner phase-space density function inside the deuteron is obtained through its wave function by

$$\begin{aligned}\rho_\mathrm{d}^W(\mathbf{r}, \mathbf{k}) &= \int \psi\left(\mathbf{r} + \frac{\mathbf{R}}{2}\right)\psi^*\left(\mathbf{r} - \frac{\mathbf{R}}{2}\right) \\ &\quad \times \exp(-i\mathbf{k}\cdot\mathbf{R})\mathrm{d}^3\mathbf{R} \\ &= 8\exp\left(-\frac{\mathbf{r}^2}{\sigma_\mathrm{d}^2} - \sigma_\mathrm{d}^2\mathbf{k}^2\right),\end{aligned} \tag{21}$$

where $\mathbf{k} = (\mathbf{k}_1 - \mathbf{k}_2)/2$ is the relative momentum between hadrons inside deuteron.

For t, ^{3}He, $^3_\Lambda$H, their hadron wave functions, are taken to be the same and are given by that of a spherical harmonic oscillator as well [28, 37], that is,

$$\psi(\mathbf{r}_1, \mathbf{r}_2, \mathbf{r}_3) = \left(3\pi^2 b^4\right)^{-3/4}\exp\left(-\frac{\rho^2 + \lambda^2}{2b^2}\right). \tag{22}$$

The ρ, λ, b, respectively, denotes the relative coordinates and size parameter. The Usual Jacobi coordinates for a three-hadrons system [34, 35] was used in Eq. (22), that is,

$$\begin{pmatrix}\mathbf{R} \\ \rho \\ \lambda\end{pmatrix} = \begin{pmatrix}\frac{1}{3} & \frac{1}{3} & \frac{1}{3} \\ \frac{1}{\sqrt{2}} & -\frac{1}{\sqrt{2}} & 0 \\ \frac{1}{\sqrt{6}} & \frac{1}{\sqrt{6}} & -\frac{2}{\sqrt{6}}\end{pmatrix}\begin{pmatrix}\mathbf{r}_1 \\ \mathbf{r}_2 \\ \mathbf{r}_3\end{pmatrix}, \tag{23}$$

where $\mathbf{R}$ denotes the center-of-mass coordinate of the three hadrons inside the cluster, and $\mathbf{r}_1$, $\mathbf{r}_2$, $\mathbf{r}_3$ are, respectively, the coordinates of the three hadrons inside cluster.

According to the following relation,

$$(\mathbf{r}_1-\mathbf{R})^2+(\mathbf{r}_2-\mathbf{R})^2+(\mathbf{r}_3-\mathbf{R})^2=\rho^2+\lambda^2, \tag{24}$$

the root-mean-square radius R_3 of a three-cluster is given by

$$R_3=\left[\int\frac{\rho^2+\lambda^2}{3}|\psi(\mathbf{r}_1,\mathbf{r}_2,\mathbf{r}_3)|^2 3^{3/2}\mathrm{d}\rho\mathrm{d}\lambda\right]^{1/2} =b. \tag{25}$$

The hadron Wigner phase-space function inside the three-hadrons cluster is obtained from its hadron wave function via

$$\begin{aligned}\rho_3^W=&\int\psi\left(\rho+\frac{\mathbf{R_1}}{2},\lambda+\frac{\mathbf{R_2}}{2}\right)\psi^*\left(\rho-\frac{\mathbf{R_1}}{2},\lambda-\frac{\mathbf{R_2}}{2}\right)\\&\times\exp\left(-i\mathbf{k}_\rho\cdot\mathbf{R_1}\right)\exp(-i\mathbf{k}_\lambda\cdot\mathbf{R_2})3^{3/2}\mathrm{d}\mathbf{R_1}\mathrm{d}\mathbf{R_2}\\=&8^2\exp\left(-\frac{\rho^2+\lambda^2}{b^2}\right)\exp\left[-\left(\mathbf{k}_\rho^2+\mathbf{k}_\lambda^2\right)b^2\right],\end{aligned} \tag{26}$$

in this equation, $\mathbf{k}_\rho$ and $\mathbf{k}_\lambda$ are relative momenta, which together with the total momentum $\mathbf{K}$ are defined by [34, 35]

$$\begin{pmatrix}\mathbf{K}\\ \mathbf{k}_\rho\\ \mathbf{k}_\lambda\end{pmatrix}=\begin{pmatrix}1 & 1 & 1\\ \frac{1}{\sqrt{2}} & -\frac{1}{\sqrt{2}} & 0\\ \frac{1}{\sqrt{6}} & \frac{1}{\sqrt{6}} & -\frac{2}{\sqrt{6}}\end{pmatrix}\begin{pmatrix}\mathbf{k}_1\\ \mathbf{k}_2\\ \mathbf{k}_3\end{pmatrix}, \tag{27}$$

with $\mathbf{k}_1$, $\mathbf{k}_2$, $\mathbf{k}_3$ being the momenta of the three hadrons.

The root-mean-square radii are 1.92, 1.61, 1.74, and 5 fm for d, t, ^{3}He, and $^3_\Lambda$H [1, 28], respectively. The information about time-space and energy-momentum of hadrons (proton, neutron, lambda) can be produced by ART 1.0 model. The overlapping Wigner phase-space density can be calculated using time-space and energy-momentum distribution of hadrons by Eqs. (21) and (26) for a two-hadrons cluster system and a three-hadrons cluster system, respectively. Using Wigner phase-space density information, the multiplicity of these clusters can be calculated by Eq. (19).

4 Results and discussions

4.1 Rapidity distributions and inclusive yields

We investigate the rapidity distributions of light nuclei and light hypernuclei including p, n, Λ, ^{2}H, ^{3}H, ^{3}He, $^3_\Lambda$H, using the ART 1.0 model coupled with a dynamical

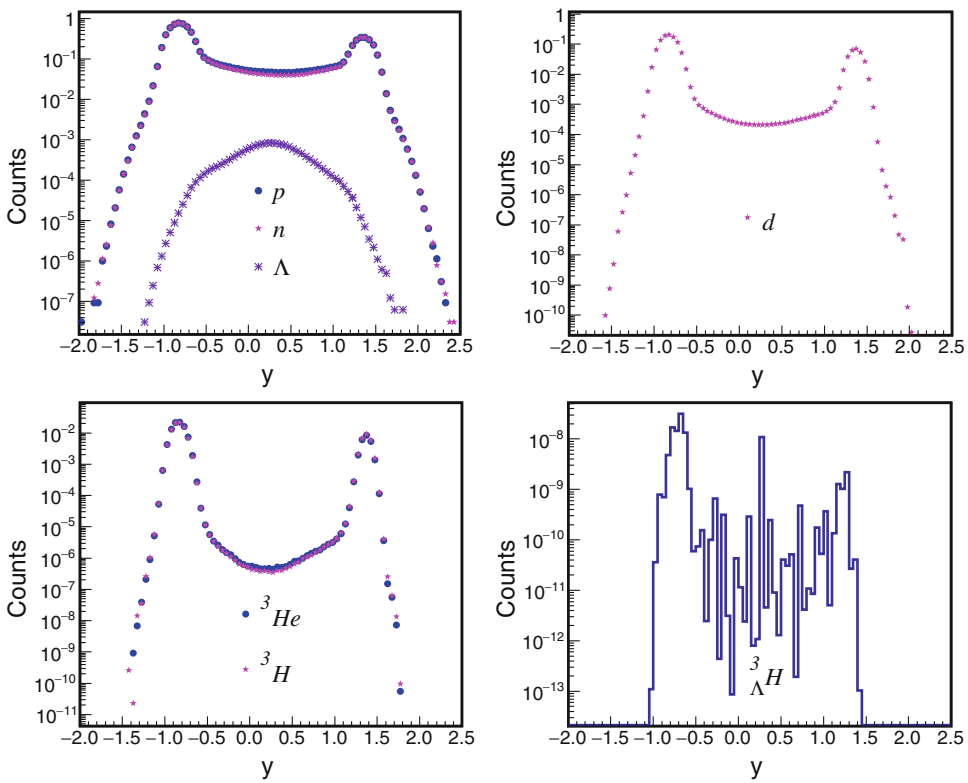

Fig. 1 (Color online) The rapidity y distributions of p, n, Λ, ^{2}H, ^{3}H, ^{3}He, and $^3_\Lambda$H in the system of center-of-mass and in minimum bias (0–80% centrality) ^{6}Li + ^{12}C reactions at beam energy of 3.5*A* GeV. Projectile beam direction is the positive direction. The distributions were normalized to one event

coalescence model. Figure 1 shows the rapidity distributions of these nuclei and hypernuclei in 0–80% centrality ^{6}Li + ^{12}C reactions at beam energy of 3.5A GeV. As showed in Fig. 1, protons and neutrons have the same distribution and mainly distributed at forwards and backwards of rapidity, but, Λ mainly distributed at middle rapidity region. Deuteron, triton, and helium distributions of rapidity are similar to the proton and neutron distributions because these light clusters are coalesced by protons and neutrons. $^{3}_{\Lambda}$H is coalesced by nucleons and Λs. As observed in Fig. 1, its rapidity distribution is mainly at forwards, backwards, and middle rapidity region because of Λ's rapidity as a factor impacting the rapidity distributions of $^{3}_{\Lambda}$H. Additionally, we can find from Fig. 1 that there are more $^{3}_{\Lambda}$H at the forwards and backwards rapidity region than the middle rapidity region, but more Λ distributed at middle rapidity region than the forwards and backwards rapidity region. This phenomenon can be explained by a possible mechanism of $^{3}_{\Lambda}$H formation by a proton and a neutron from spectator to capture a Λ, or a deuteron coalesced by a proton and a neutron from spectator to capture a Λ. Some theorists have studied this mechanism with other models [38, 39].

The inclusive yields of p, n, Λ, ^{2}H, ^{3}H, ^{3}He, $^{3}_{\Lambda}$H are also calculated. Our results are 9.007, 8.792, 0.015, 1.259, 0.109, 0.110, and 1.023×10^{-7} for p, n, Λ, ^{2}H, ^{3}H, ^{3}He, and $^{3}_{\Lambda}$H in centrality 0–80% ^{6}Li + ^{12}C reactions at the beam energy of 3.5A GeV from ART 1.0 model coupled with a dynamical coalescence model. Our results are close to the experimental results in the reactions of ^{6}Li + ^{12}C at beam energy 2A GeV from the HypHI project at GSI [19]. According to the yields of $^{3}_{\Lambda}$H, it is seen that the future facility is suitable for studying the hypernuclear physics when HIAF is built completely.

4.2 Penalty factor and θ distributions versus rapidity

The yields of light clusters are exponentially dependent on the nuclear mass number. Figure 2 shows the relations between yields and the nuclear mass number. The line in Fig. 2 is the fit function as the following [40]:

$$N_A = N_{\mathrm{p}}^{i}\left(\frac{1}{\lambda_0}\right)^{A-1}. \tag{28}$$

N_A denotes the yields of light clusters with nuclear mass number A, N_{p}^{i} is the total mass number of initial protons, A is the nuclear mass number, and λ_0 is called as penalty factor.

Penalty factor is used to quantitatively describe the difficulty that nucleons produce the next massive cluster with nuclear mass number $A + 1$ compared with the current cluster with nuclear mass number A. We know from Eq. (28) that, if penalty factor is smaller, it is easier to form a light cluster by protons and neutrons. Equation (28) can be used to estimate the production rates of nuclear cluster systems with nuclear mass number A. We calculated the penalty factor at different region of rapidity in center-of-mass frame and in centrality 0–80% ^{6}Li + ^{12}C reactions at beam energy 3.5A GeV. The penalty factor is 5.387, 132.371, 6.103 at the region of rapidity −2.0 to −0.5, −0.5 to 1.0, 1.0 to 2.5 as showed in Fig. 2, respectively. According to our calculation, the penalty factor at the backwards and forwards rapidity region is smaller than at the middle rapidity region, therefore, the formation of light cluster nuclei is easier at the forwards and backwards rapidity regions than at the middle rapidity region. In peripheral relativistic ion collisions, there are more spectators than there are in the central relativistic ion collisions. Spectator will have higher rapidity, and more light clusters may be produced at peripheral relativistic heavy-ion collisions [39].

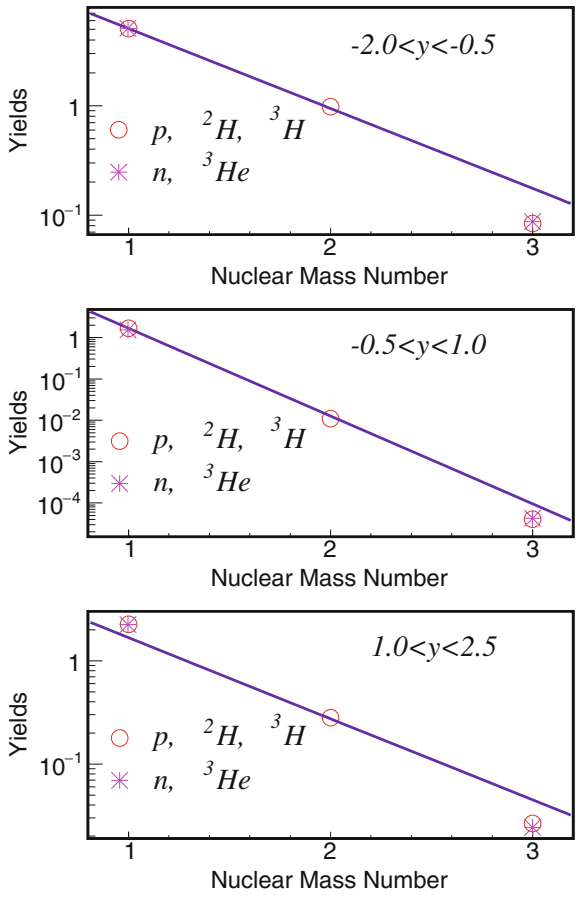

Fig. 2 (Color online) The yields of light clusters as a function of the nuclear mass number at a different region of rapidity in the center-of-mass frame and in minimum bias (0–80% centrality) ^{6}Li + ^{12}C reactions at beam energy of 3.5A GeV

The θ angle, which is the angle between the momentum of particles produced in the collisions and the projectiles beam direction, provides a direct guide on detector acceptance for experimentalist. Figure 3 shows the θ distributions for p, n, and Λ, respectively. We can see from Fig. 3 that protons and neutrons are mainly at the near angle of π and 0. Λs are different from protons and neutrons, which mainly distribute at the middle angle between 0.5 and 2.5. One can learn from Fig. 3 that the θ is directly related to rapidity of a particle, and a particle must be at the θ near π and 0 with forwards and backwards rapidity. According to the θ versus rapidity distributions (Fig. 3 of nucleons) and the rapidity distributions (Fig. 1), the optimal place for the light nuclear cluster and hypernuclei ${}^{3}_{\Lambda}$H in HIAF will appear at the θ near π and 0 region. The conventional gas chamber detector will capture the trajectory of charged nuclei while for the neutral particle, special detectors are required [40].

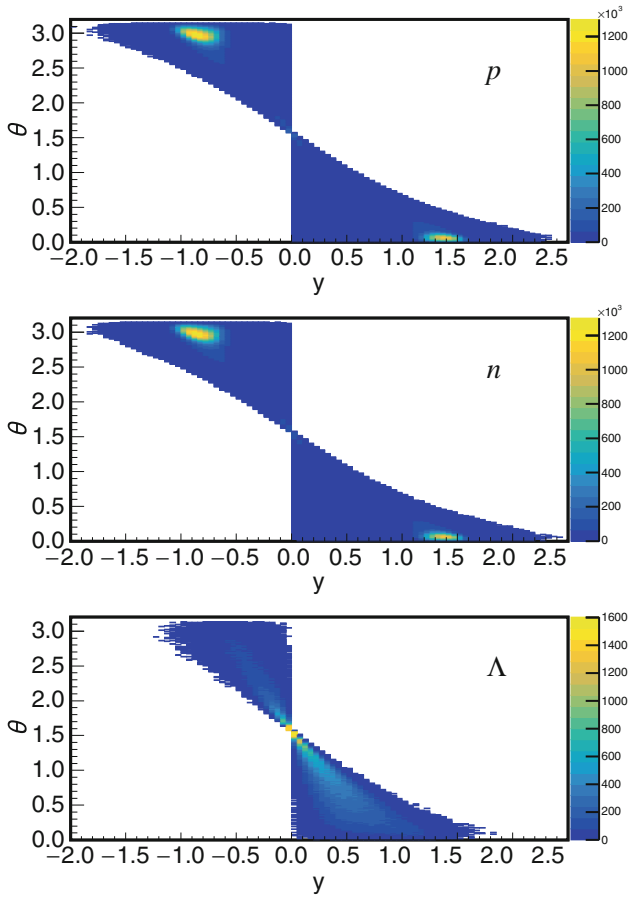

Fig. 3 (Color online) The θ versus rapidity distributions in the system of center-of-mass frame and in minimum bias (0–80% centrality) ^{6}Li + ^{12}C reactions at beam energy of 3.5*A* GeV for p, n, and Λ, respectively

5 Summary

In this paper, we calculated the yields of light nuclear clusters and light hyperneuclei in centrality 0–80% ^{6}Li + ^{12}C reactions at beam energy 3.5*A* GeV from ART 1.0 model plus a dynamical coalescence model. The inclusive yields are 9.007, 8.792, 0.015, 1.259, 0.109, 0.110 and 1.023×10^{-7} for p, n, Λ, ^{2}H, ^{3}H, ^{3}He, and ${}^{3}_{\Lambda}$H, respectively. We also investigate the penalty factor for light nuclear clusters at the projectile/target rapidity region and middle rapidity region, respectively. A proposal at where the particle detector should be placed was made. Our study shows that HIAF is suitable for light nuclei and hypernuclei study.

Acknowledgements We are grateful for the discussion with Dr. T. Saito.

References

1. T.A. Armstrong, K.N. Barish, S. Batsouli et al., Production of ${}^{3}_{\Lambda}H$ and ${}^{4}_{\Lambda}H$ in central 11.5 GeV/*c* Au + Pt heavy ion collisions. Phys. Rev. C **70**, 024902 (2004). doi:10.1103/PhysRevC.70.024902
2. D. Lonardoni, A. Lovato, S. Gandolfi et al., Hyperon puzzle: hints from quantum monte carlo calculations. Phys. Rev. Lett. **114**, 092301 (2015). doi:10.1103/PhysRevLett.114.092301
3. J.M. Lattimer, M. Prakash, The physics of neutron stars. Science **304**, 536 (2004). doi:10.1126/science.1090720
4. R.H. Dalitz, G. Rajasekharan, The spins and lifetimes of the light hypernuclei. Phys. Lett. **1**, 58–60 (1962). doi:10.1016/0031-9163(62)90437-7
5. H. Kamada, J. Golak, K. Miyagawa et al., π-mesonic decay of the hypertriton. Phys. Rev. C **57**, 1595–1603 (1998). doi:10.1103/PhysRevC.57.1595
6. M. Juric, G. Bohm, J. Klabuhn et al., A new determination of the binding-energy values of the light hypernuclei (A $\leq$ 15). Nucl. Phys. B **52**, 1–30 (1973). doi:10.1016/0550-3213(73)90084-9
7. S. Zhang, J.H. Chen, Y.G. Ma et al., Hypertriton and light nuclei production at Λ-production subthreshold energy in heavy-ion collisions. Chin. Phys. C (HEP&NP) **35**(8), 741–747 (2011). doi:10.1088/1674-1137/35/8/008
8. Z.Q. Zhang, Y.G. Ma, Measurements of momentum correlation and interaction parameters between antiprotons. Nucl. Sci. Tech. **27**, 152 (2016). doi:10.1007/s41365-016-0147-x
9. L. Adamczyk, S.T.A.R. Collaboration et al., Measurement of interaction between antiprotons. Nature **527**, 345–348 (2015). doi:10.1038/nature15724
10. H. Agakishiev, STAR Collaborationm et al., Observation of the antimatter helium-4 nucleus. Nature **473**, 353–356 (2011). doi:10.1038/nature10079
11. L. Xue, STAR Collaboration, Observation of the antimatter helium-4 nucleus at the RHIC. J. Phys. G Nucl. Part. Phys. **38**, 124072 (2011). doi:10.1088/0954-3899/38/12/124072
12. Y.F. Xu, Y.J. Ye, J.H. Chen et al., Low-mass vector meson production at forward rapidity in p + p and d + Au collisions at $\sqrt{S_{NN}}$ = 200 GeV from a multiphase transport model. Nucl. Sci. Tech. **27**, 87 (2016). doi:10.1007/s41365-016-0093-7
13. L. Adamczyk, STAR Collaboration et al., $\Lambda\Lambda$ correlation function in Au + Au collisions at $\sqrt{S_{NN}}$ = 200 GeV. Phys. Rev. Lett. **114**, 022301 (2015). doi:10.1103/PhysRevLett.114.022301

14. Y.G. Ma, J.H. Chen, L. Xue, A brief review of antimatter production. Front. Phys. **7**, 637 (2012). doi:10.1007/s11467-012-0273-9
15. Y.G. Ma, J.H. Chen, L. Xue et al., Hunting antimatter nuclei in ultrarelativistic heavy-ion collisions. Nucl. Phys. News **23**(1), 10–14 (2013). doi:10.1080/10619127.2012.738164
16. B.I. Abelev, STAR Collaboration et al., Observation of an antimatter hypernucleus. Science **328**, 58–62 (2010). doi:10.1126/science.1183980
17. J.H. Chen, STAR Collaboration, Observation of hypertritons in Au+Au collisions at $\sqrt{S_{NN}}$ = 200 GeV. Nucl. Phys. A **830**, 761c–764c (2009). doi:10.1016/j.nuclphysa.2009.10.001
18. R. Lea et al., Hypernuclei production in Pb-Pb collisions at $\sqrt{S_{NN}}$ = 2.76 TeV with ALICE at the LHC. Nucl. Phys. A **914**, 415–420 (2013). doi:10.1016/j.nuclphysa.2013.02.089
19. C. Rappold, E. Kim, D. Nakajima et al., Hypernuclear spectroscopy of products from ^{6}Li projectiles on a carbon target at 2 *A* GeV. Nucl. Phys. A **913**, 170–184 (2013). doi:10.1016/j.nuclphysa.2013.05.019
20. See details of a topical session at HYP2015 International Conference, http://lambda.phys.tohoku.ac.jp/hyp2015/
21. A. Feliciello, Recent achievements in hypernuclear physics. Few Body Syst. **55**, 605–613 (2014). doi:10.1007/s00601-013-0759-1
22. N. Shah, Y.G. Ma, J.H. Chen et al., Production of multistrange hadrons, light nuclei and hypertriton in central Au + Au collisions at $\sqrt{S_{NN}}$ = 11.5 and 200 GeV. Phys. Lett. B **754**, 6–10 (2016). doi:10.1016/j.physletb.2016.01.005
23. T.Z. Yan, Y.G. Ma, X.Z. Cai et al., Scaling of anisotropic flow and momentum-space densities for light particles in intermediate energy heavy ion collisions. Phys. Lett. B **638**, 50–54 (2006). doi:10.1016/j.physletb.2006.05.018
24. G.F. Bertsch, S. Das, Gupta, A guide to microscopic models for intermediate energy heavy ion collisions. Phys. Rep. **160**, 189–233 (1988). doi:10.1016/0370-1573(88)90170-6
25. B.A. Li, W. Bauer, Two-temperature shape of pion spectra in relativistic heavy-ion reactions. Phys. Lett. B **254**, 335–339 (1991). doi:10.1016/0370-2693(91)91165-R
26. W.Z. Lin, C.M. Ko, B.A. Li et al., Multiphase transport model for relativistic heavy ion collisions. Phys. Rev. C **72**, 064901 (2005). doi:10.1103/PhysRevC.72.064901
27. B.A. Li, C.M. Ko, Formation of superdense hadronic matter in high energy heavy-ion collisions. Phys. Rev. C **52**, 2037–2063 (1995). doi:10.1103/PhysRevC.52.2037
28. M. Gyulassy, K. Frankel, E.A. Relmer, Deuteron formation in nuclear collisions. Nucl. Phys. A **402**, 596–611 (1983). doi:10.1016/0375-9474(83)90222-1
29. S. Zhang, J.H. Chen, H. Crawford et al., Searching for onset of deconfinement via hypernuclei and baryon-strangeness correlations. Phys. Lett. B **684**, 224–227 (2010). doi:10.1016/j.physletb.2010.01.034
30. R. Mattiello, H. Sorge, H. Stocker et al., Nuclear clusters as a probe for expansion flow in heavy ion reactions at (10–15)*A* GeV. Phys. Rev. C **55**, 1443–1454 (1997). doi:10.1103/PhysRevC.55.1443
31. Y. Oh, C.M. Ko, Elliptic flow of deuterons in relativistic heavy-ion collisions. Phys. Rev. C **76**, 054910 (2007). doi:10.1103/PhysRevC.76.054910
32. K.J. Sun, L.W. Chen, Production of antimatter ^{5,6}Li nuclei in central Au + Au collisions at $\sqrt{S_{NN}}$ = 200 GeV. Phys. Lett. B **751**, 272–277 (2015). doi:10.1016/j.physletb.2015.10.056
33. R. Mattiello, A. Jahns, H. Sorge et al., Deuteron flow in ultrarelativistic heavy ion reactions. Phys. Rev. Lett. **74**, 2180–2183 (1995). doi:10.1103/PhysRevLett.74.2180
34. L.W. Chen, C.M. Ko, B.A. Li, Light clusters production as a probe to nuclear symmetry energy. Phys. Rev. C **68**, 017601 (2003). doi:10.1103/PhysRevC.68.017601
35. L.W. Chen, C.M. Ko, B.A. Li, Light cluster production in intermediate energy heavy-ion collisions induced by neutron-rich Nuclei. Nucl. Phys. A **729**, 809 (2003). doi:10.1016/j.nuclphysa.2003.09.010
36. A. Polleri, R. Mattiello, I.N. Mishustin et al., Reconstruction of the proton source in relativistic heavy ion collisions. Nucl. Phys. A **661**, 452–455 (1999). doi:10.1016/S0375-9474(99)85063-5
37. A.T.M. Aerts, C.B. Dover, On the production of the six-quark *H* dibaryon in the (K^-, K^+) reaction. Phys. Rev. D **28**, 450–463 (1983). doi:10.1103/PhysRevD.28.450
38. A.S. Botvina, J. Steinheimer, E. Bratkovskaya et al., Formation of hypermatter and hypernuclei within transport models in relativistic ion collisions. Phys. Lett. B **742**, 7–14 (2015). doi:10.1016/j.physletb.2014.12.060
39. A.S. Botvina, K.K. Gudima et al., Production of hypernuclei in peripheral relativistic ion collisions. Phys. Rev. C **88**, 054605 (2013). doi:10.1103/PhysRevC.88.054605
40. Z.B. Xu, Search for positively charged strangelets and other related results with E864 at the AGS. J. Phys. G Nucl. Part. Phys. **25**, 403 (1999). doi:10.1088/0954-3899/25/2/029